Cell Transplantation, Vol. 26, pp. 215–228, 2017

0963-6897/17 $90.00 + .00
DOI: https://doi.org/10.3727/096368916X692951
E-ISSN 1555-3892
www.cognizantcommunication.com

A Nerve Conduit Containing a Vascular Bundle and Implanted With Bone Marrow Stromal Cells and Decellularized Allogenic Nerve Matrix

Yukitoshi Kaizawa,* Ryosuke Kakinoki,† Ryosuke Ikeguchi,* Soichi Ohta,* Takashi Noguchi,* Hisataka Takeuchi,* Hiroki Oda,* Hirofumi Yurie,* and Shuichi Matsuda*

*Department of Orthopaedic Surgery, Graduate School of Medicine, Kyoto University, Kyoto, Japan
†Department of Orthopaedic Surgery, Faculty of Medicine, Kindai University, Sayama, Osaka, Japan

Cells, scaffolds, growth factors, and vascularity are essential for nerve regeneration. Previously, we reported that the insertion of a vascular bundle and the implantation of bone marrow-derived mesenchymal stem cells (BM-MSCs) into a nerve conduit promoted peripheral nerve regeneration. In this study, the efficacy of nerve conduits containing a vascular bundle, BM-MSCs, and thermally decellularized allogenic nerve matrix (DANM) was investigated using a rat sciatic nerve model with a 20-mm defect. Lewis rats were used as the sciatic nerve model and for the preparation of BM-MSCs, and Dark Agouti rats were used for the preparation of the DANM. The revascularization and the immunogenicity of the DANM were investigated histologically. The regeneration of nerves through nerve conduits containing vessels, BM-MSCs, and DANM (VBD group) was evaluated based on electrophysiological, morphometric, and reinnervated muscle weight measurements and compared with that of vessel-containing conduits that were implanted with BM-MSCs (VB group). The DANM that was implanted into vessel-containing tubes (VCTs) was revascularized by neovascular vessels that originated from the inserted vascular bundle 5–7 days after surgery. The number of $CD8^+$ cells found in the DANM in the VCT was significantly smaller than that detected in the untreated allogenic nerve segment. The regenerated nerve in the VBD group was significantly superior to that in the VB group with regard to the amplitude of the compound muscle action potential detected in the pedal adductor muscle; the number, diameter, and myelin thickness of the myelinated axons; and the tibialis anterior muscle weight at 12 and 24 weeks. The additional implantation of the DANM into the BM-MSC-implanted VCT optimized the axonal regeneration through the conduit. Nerve conduits constructed with vascularity, cells, and scaffolds could be an effective strategy for the treatment of peripheral nerve injuries with significant segmental defects.

Key words: Peripheral nerve injury; Vascularity; Allogenic nerve tissue; Nerve conduit; Bone marrow-derived mesenchymal stem cells (BM-MSCs)

INTRODUCTION

Currently, several artificial nerve conduits are commercially available for the repair of peripheral nerve injuries with segmental defects. However, their clinical use is limited mainly to the repair of sensory nerves with small defects (<3 cm) and a small caliber, such as the digital nerves of the fingers[1,2]. To extend the application of artificial nerves clinically, various modifications have been performed on common hollow tubes in recent decades. Nevertheless, in the present clinical settings, autologous nerve grafting remains the gold standard for the repair of peripheral nerve defects.

We have reported the efficacy of the addition of vascularity and cellular components to nerve-guiding tubes. Our previous study demonstrated that nerve regeneration through a nerve-guiding silicone tube was accelerated by the insertion of blood vessels into the tube [vessel-containing tube (VCT)][3]. We also showed that the implantation of bone marrow-derived mesenchymal stem cells (BM-MSCs) into the VCT optimized axonal regeneration in a rat sciatic nerve model with a 15-mm defect[4]. In a recent study, we used a canine model with a 30-mm gap in the ulnar nerve and observed successful nerve regeneration through a VCT with BM-MSC implantation. However, it was also shown that nerve regeneration within the tube remained inferior to that detected through a 30-mm autogenous nerve graft[5]. We considered that the lack of a scaffold, which would

Received February 25, 2016; final acceptance December 7, 2016. Online prepub date: September 21, 2016.
Address correspondence to Ryosuke Kakinoki, Department of Orthopaedic Surgery, Faculty of Medicine, Kindai University, 377-2 Oono-higashi, Osaka-sayama, Osaka 589-8511, Japan. Tel: +81-72-366-0221; Fax: +81-72-366-0206; E-mail: rkakinoki@med.kindai.ac.jp *or* kaizawa@kuhp.kyoto-u.ac.jp

facilitate Schwann cell migration and axonal extension and trap the implanted BM-MSCs within the lumen of the tube, might be one of the causes of the inferior nerve regeneration observed through the tube.

Recently, several authors have demonstrated the successful preservation of extracellular matrix (ECM) components and the reduction of the immunogenicity of the allogenic nerve tissue after thermal decellularization (freezing and thawing)[6–11]. A decellularized allogenic nerve matrix (DANM) is a useful source of a scaffold for peripheral nerve regeneration because a preserved ECM functions as a three-dimensional (3D) scaffold. In addition, DANM transplantation was not associated with size and volume limitations or donor site morbidity.

In the present study, we created a tube containing a vascular pedicle, BM-MSCs, and a DANM. First, we investigated the revascularization and the immunogenicity of the DANM that was implanted together with a vascular bundle that was inserted in the tube. Moreover, nerve regeneration in the VCT that was implanted with BM-MSCs and a DANM was compared with that observed in the BM-MSC-implanted VCT without DANM transplantation using a rat sciatic nerve model with a 20-mm gap. Our hypothesis was that the DANM is revascularized in the early stage of nerve regeneration and shows no harmful immunogenicity when implanted in a VCT and that additional DANM transplantation into the BM-MSC-implanted VCT facilitates axonal regeneration compared with the BM-MSC-implanted VCT without DANM transplantation.

MATERIALS AND METHODS

Animals

Seventy-four female Lewis rats (RT-1^{l}; 9–11 weeks of age and weighing 180–220 g; Nippon SLC, Hamamatsu, Japan) for a sciatic nerve defect model, 2 inbred female Lewis rats (7 weeks of age and weighing 160 g; Nippon SLC) for harvest of the BM-MSCs, and 26 female Dark Agouti (DA) rats (RT-1^{a}; 9–11 weeks of age and weighing 160–180 g; Nippon SLC) for preparation of DANMs were used. All animal protocols were approved by the Animal Research Committee of Kyoto University.

Preparation of a DANM

DA rats were used as donors, and Lewis rats were used as recipients. This strain combination represents a genetic difference at both the major histocompatibility complex (MHC) and the non-MHC levels[12]. Under aseptic conditions, the bilateral sciatic nerves of anesthetized DA rats were exposed. The connective tissue of the nerves was removed, and the nerve segments were excised. The DANM was prepared via thermal extraction, and all subsequent steps were conducted based on a protocol that was developed previously[6–11]. Briefly, nerve tissues were immersed in liquid nitrogen until thermal equilibrium was achieved and were then placed into phosphate-buffered saline (PBS) at room temperature (RT) for 2 min. This freezing and thawing cycle was repeated three times. The grafts were preserved in a freezer (−20°C) until use.

Preparation of BM-MSCs

BM-MSCs were obtained from 7-week-old female Lewis rat femoral and tibial bones, as reported previously[4,13]. Briefly, the distal and proximal ends of the femoral and tibial bones were removed to expose bone marrow cavities. Mesenchymal cell growth medium (α-MEM; Gibco, Palo Alto, CA, USA) supplemented with 10% fetal bovine serum (FBS) and 1% penicillin–streptomycin (Sigma-Aldrich, St. Louis, MO, USA) was injected through each cavity using a 21-gauge needle. The resulting cell suspension was filtered through a 70-μm Falcon™ cell strainer (Corning, Corning, NY, USA) and centrifuged for 5 min at $120 \times g$. The supernatant was aspirated, and the cell boluses were resuspended in mesenchymal cell growth medium (α-MEM + FBS + penicillin–streptomycin), plated in 75-cm^2 tissue culture flasks, and incubated in 5% CO_2 at 37°C. The nonadherent cells were removed after 48 h. Thereafter, the mesenchymal cell growth medium was replaced with fresh medium every 3 days. The cells were allowed to grow to 80%–85% confluence, at which point the cultures were treated with a trypsin–ethylenediaminetetraacetic acid (EDTA) solution (0.25% trypsin, 0.02% EDTA; Sigma-Aldrich) and were then harvested and diluted to 1:4 per passage, for further expansion. Cells at passages 5–7 were used in the experiments[4,14].

Experimental Design and Groups

Seventy-four female Lewis rats were divided into six groups. Table 1 provides an overview of the groups and experimental design used in this study. The 20-mm gaps in the rat sciatic nerves were repaired with (i) vessel-containing silicone tubes with implantation of BM-MSCs and a DANM (VBD group, $n = 22$), (ii) vessel-containing silicone tubes supplemented with BM-MSCs (VB group, $n = 16$), (iii) VCTs with implantation of a DANM (VD group, $n = 12$), (iv) silicone tubes containing a DANM (D group, $n = 12$), (v) fresh allogenic nerve grafts (allo group, $n = 6$), or (vi) autologous nerve grafts (auto group, $n = 6$).

The revascularization and the immunogenicity of the DANM in VCTs (VD group, $n = 12$) were evaluated histologically and compared with those observed in the D group ($n = 12$, negative control) at 5, 7, 14, and 28 days, and with those recorded in the allo group ($n = 6$, positive control) and the auto group ($n = 6$, negative control) at 14 and 28 days, respectively. The midportion of the

Table 1. Experimental Design and Number of Animals in Each Group

	5 Days	1 Week	2 Weeks	4 Weeks	6 Weeks	12 Weeks	24 Weeks
Groups							
VBD (vessel-containing tube with implantation of BM-MSCs and DANM)					6	8	8
VB (vessel-containing tube with BM-MSC implantation)8						8	8
D (silicon tube with DANM implantation)	3	3	3	3			
VD (vessel-containing tube with DANM implantation)	3	3	3*	3*			
Allo (allogenic nerve graft)			3	3			
Auto (autologous graft)			3	3			
Evaluations							
Revascularization of the DANM (D group vs. VD group)	6	6	6	6			
Immunogenicity of the DANM (VD group vs. allo group vs. auto group)			9	9			
Differentiation of the implanted BM-MSCs (VBD group)					6		
Nerve regeneration (VBD group vs VB group)						16	16

*In the VD group at 2 and 4 weeks, the middle and the distal portion of the DANM were harvested from each rat and used for the evaluation of the revascularization and the immunogenicity, respectively.

DANM was assessed for revascularization (VD group, $n=12$ vs. D group, $n=12$), and the distal portion of the DANM was used for the evaluation of immunogenicity (VD group, $n=6$ vs. allo group, $n=6$ vs. auto group, $n=6$). Nerve regeneration was assessed in 16 rats in the VBD group at 12 and 24 weeks after surgery and compared with that observed in the VB group ($n=16$). The capability of differentiation of the implanted BM-MSCs into Schwann cell-like cells was also examined at 6 weeks in six rats from the VBD group.

Surgical Procedures

VBD Group ($n=22$). The right sciatic nerve was exposed from the sciatic notch to the popliteal fossa using a gluteal muscle-splitting approach under general anesthesia with intraperitoneally injected sodium pentobarbital (60 mg/kg). A 15-mm segment of the sciatic nerve was removed at the mid-thigh level. An additional skin incision of 3 cm was performed from the popliteal fossa to the ankle. The sural nerve was transected just distal to its trifurcation from the sciatic nerve at the popliteal fossa and at the ankle, separated from its concomitant vessels (sural vessels), and removed completely. A 0.5×0.5-cm myocutaneous flap that was vascularized by the sural vessels was elevated from the posterior surface of the hindlimb. The pedicled myocutaneous flap was turned proximal to the origin of the sural vessels from the popliteal vessels as a pivotal point[3,4] (Fig. 1A and B). A 20-mm DANM was implanted between the transected sciatic nerve stumps using two 10/0 monofilament nylon sutures under an operating microscope. The DANM with the adjacent sciatic nerve stumps was then inserted into a 23-mm silicone rubber tube (outer diameter, 3.0 mm; inner diameter, 2.0 mm; Dow Corning, Midland, MI, USA) through its longitudinal slit, with the epineuria of the proximal and distal sciatic nerve stumps anchored to the lumen by 9-0 nylon sutures (Fig. 1C and C′). Subsequently, the sural vessels were inserted into the silicone tube through its longitudinal slit. The expected roles of the wrapping of the silicone tube around the DANM included the prevention of scarring and of the formation of adhesions around the regenerating nerve, and the generation of an appropriate environment for peripheral nerve regeneration inside the lumen. After the insertion of the sural vessels and the implantation of the DANM, the longitudinal slit of the tube was closed using several stitches of 5-0 nylon suture to reduce the possibility of extra leakage of trophic, cellular, and humoral factors through the slit (Fig. 1D and D′). BM-MSCs in 0.075 ml of α-MEM solution at a concentration of 3×10^7 cells/ml[15] were injected into the space surrounding the DANM inside the lumen of the tube using a 27-gauge needle[16] (Fig. 1E and E′). During the injection procedure, meticulous care was taken to avoid leaving any air in the lumen of the tube. Because some leakage from the distal end of the tube was inevitable, we injected a larger volume of the BM-MSC-containing medium than that necessary to fill the lumen of the tube. The wound was closed with 4-0 nylon sutures in layers. The myocutaneous flaps were sutured to the buttocks when closing the wound and were used as monitor flaps to indicate whether the inserted sural vessels remained patent (Fig. 1F).

VB Group ($n=16$). After the removal of a 15-mm sciatic nerve segment, the proximal and distal nerve stumps were secured 1.5 mm into the 23-mm silicone tube, which created a 20-mm interstump gap. Subsequently, the sural vessels were inserted into the tube, and BM-MSCs were injected into the lumen of the tube, as described previously[4].

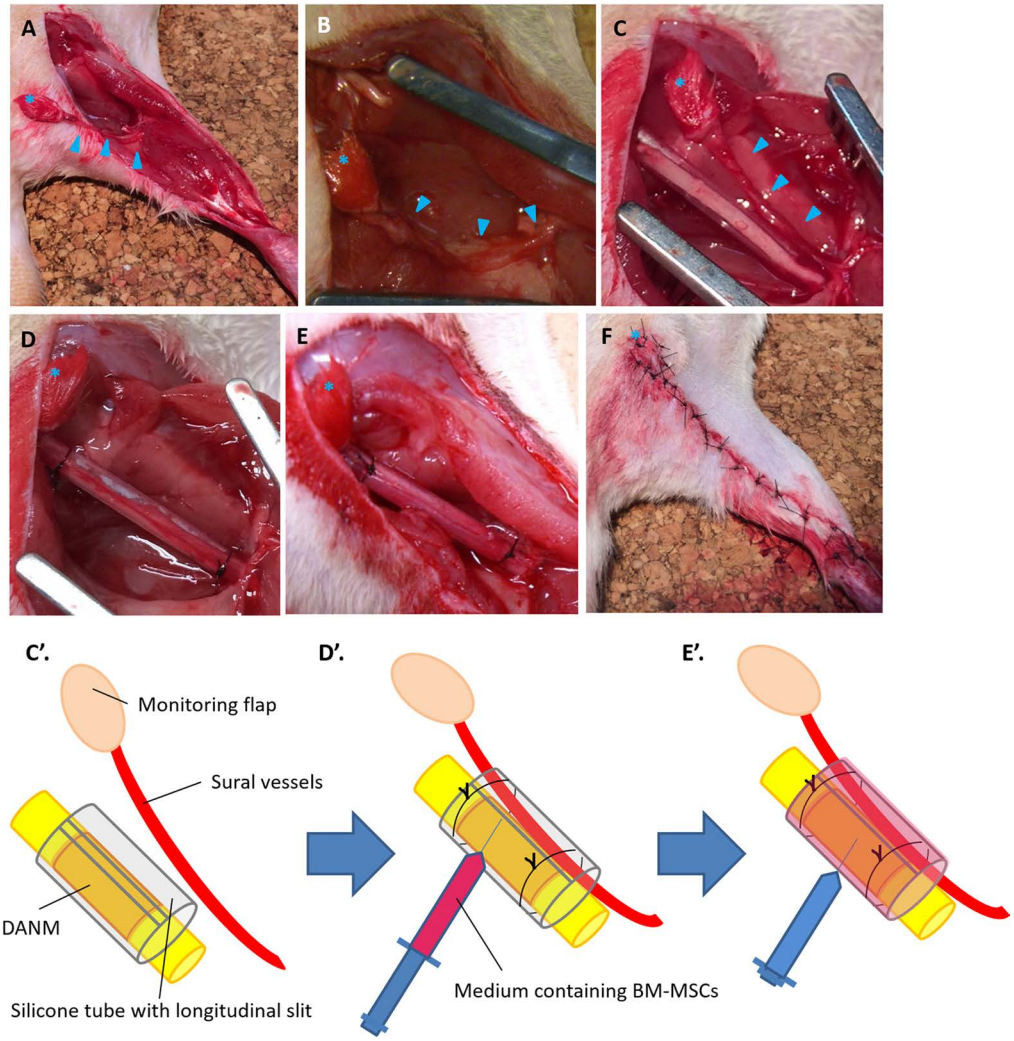

Figure 1. Surgical procedures used in the group with implantation of sural vessels, BM-MSCs, and a DANM (VBD group). (A, B) The sural flap was elevated, and a 15-mm nerve segment was resected. (C, C′) The defect was bridged by a 20-mm decellularized allogenic nerve matrix (DANM) and subsequently inserted into a silicone tube through a slit in the tube. (D, D′) A vascular pedicle with its monitoring flap was inserted into the silicon tube through the slit, and the slit was closed using 5-0 nylon suture. (E, E′) α-MEM containing bone marrow-derived mesenchymal stem cells (BM-MSCs) was injected into the tube. (F) Postoperative appearance of the limb. The arrowheads indicate vascular bundles. The asterisk indicates the monitoring flap.

VD Group (n = 12). The gap was repaired with a 20-mm DANM in a silicone tube, followed by the insertion of the sural vessels into the tube, as explained above.

D Group (n = 12). The nerve gap was bridged with a 20-mm DANM in the silicone tube, as described above.

Allo Group (n = 6). The gap was bridged with a 20-mm nerve segment that had been obtained from a DA rat sciatic nerve, without any modification.

Auto Group (n = 6). In this group, a 20-mm segment of the sciatic nerve was resected when creating a gap. The nerve segment was turned in the opposite direction and sutured in situ (reversed autograft).

Evaluation of the Revascularization of the DANM in the VCT (VD Group vs. D Group)

To investigate the effect of the inserted vascular bundle on the revascularization of the DANM in the silicone tube, the process of blood vessel formation in the DANM in the VD group was compared with that observed in the D group. At 5, 7, 14, and 28 days, three rats each from the VD and D groups were sacrificed, and the repaired sciatic nerve was exposed (Table 1). The silicone tube was removed carefully, and the midportion of the DANM was harvested, because revascularization in the midportion of the lumen is less affected by capillaries that extend from both ends of the tube. The

segments were fixed in 4% paraformaldehyde (PFA) (Nacalai Tesque, Kyoto, Japan) in 0.1 M phosphate buffer (PB; pH 7.4) overnight at 4°C. They were then cryoprotected in 20% sucrose for 48 h at 4°C. Subsequently, the sample was embedded in optimal cutting temperature (OCT) compound (Sakura Finetek, Torrance, CA, USA), and 16-μm-thick transverse frozen sections were placed onto poly-L-lysine-coated slides. After three washes with PBS, antigen retrieval was performed in proteinase K (PK; Sigma-Aldrich) at RT for 10 min. As a blocking procedure, donkey serum (Sigma-Aldrich) was added to the slides, which were then incubated at RT for 1 h. Sections were incubated at 4°C for 24 h with primary antibodies [mouse monoclonal anti-rat endothelial cell cytoplasmic antigen (RECA-1) antibodies (1:40); AbD Serotec, Kidlington, UK]. Slides were washed with PBS and incubated at RT for 1 h with secondary antibodies [donkey anti-mouse IgG (H+L) whole antibodies (1:200; CF™543 fluorescent reagents; Biotium, Fremont, CA, USA)]. After additional PBS washing, coverslips were mounted onto the slides using bicarbonate-buffered glycerol (pH 8.6), and the slides were viewed using a confocal microscope (Nikon D-Eclipse C1; Nikon, Tokyo, Japan). The negative controls included the omission of primary or secondary antibodies on parallel sections (data not shown).

Evaluation of the Immunogenicity of the DANM in the VCT (VD Group vs. Auto Group vs. Allo Group)

To investigate whether the DANM that was implanted alongside the arteriovenous bundle exhibited any harmful immunogenicity, the number of cytotoxic T cells in the DANM in the VD group was compared with that recorded in the auto group (as a negative control) and in the allo group (as a positive control). At 2 and 4 weeks, the distal third of the DANM (or of the graft) was harvested from three rats each from the VD group, the auto group, and the allo group, and 16-μm-thick longitudinal frozen sections were prepared as described above (Table 1). The sections were incubated at 4°C for 24 h with mouse monoclonal antibodies against CD8a (surface marker on cytotoxic T cells) (1:10; AbD Serotec) as primary antibodies. The secondary antibodies used were donkey anti-mouse IgG (H+L) whole antibodies (1:200; CF™488 fluorescent reagents; Biotium). The number of $CD8a^+$ cells was counted using the captured images of five random high-power fields per section.

Evaluation of Nerve Regeneration Through the BM-MSC-Supplemented VCT With or Without DANM Implantation (VBD Group vs. VB Group)

To investigate whether the additional implantation of a DANM facilitated axonal regeneration through the BM-MSC-supplemented VCT, nerve regeneration in the VBD group was compared with that observed in the VB group regarding electrophysiological, morphometric, and reinnervated muscle weight measurements.

Electrophysiological Evaluations. Twelve and 24 weeks after surgery, eight rats each from the VBD and VB groups were anesthetized. The right sciatic nerve was exposed and stimulated just distal to the piriformis muscle (S1) and at the popliteal fossa (S2) using a bipolar silver electrode. Two pairs of needle electrodes were inserted into the pedal adductor muscle to check for the presence of an evoked action potential. The motor nerve conduction velocity (MNCV) was calculated for both types of evoked action potentials stimulated at S1 and S2. The amplitude (peak to peak) of the compound muscle action potentials (CMAPs) that were evoked in the pedal adductor muscles using the supramaximal electric stimulation at the S1 point was measured. The same procedure was applied to the intact left hindlimb. CMAP amplitudes and MNCVs are expressed as a percentage of the values recorded on the contralateral healthy side[3,4,17,18].

Reinnervated Muscle Weight. The bilateral tibialis anterior muscles of the rats were dissected cleanly from the origin and insertion and were removed and weighed immediately using an electronic scale with 0.01 g precision. The results are expressed as a percentage of the values obtained for the contralateral healthy side.

Histological and Morphometric Evaluations. After the electrophysiological study, the tubes and their adjacent nerve portions were removed, fixed in 1% glutaraldehyde (Nacalai Tesque) and 1.44% PFA, postfixed in 1% osmic acid (Nacalai Tesque), and embedded in epoxy resin (Nacalai Tesque). Transverse sections (thickness, 1 μm) of the regenerating nerves were taken from the part that was 5 mm proximal to the distal sutures. The sections were stained with 0.5% (w/v) toluidine blue solution (MERCK, Darmstadt, Germany) and examined using a light microscope (Nikon ECLIPSE 80i; Nikon). The total number of regenerated myelinated axons was counted using ImageJ (NIH, http://rsbweb.nih.gov/ij/) as reported in our previous articles[3–5,17,18]. Briefly, the entire neural area (a) of each specimen was calculated on an image at a magnification of 40×. Six or seven fields were chosen at random so that the area analyzed would represent >20% of the entire neural area of each specimen. The number of myelinated axons and the neural area were calculated for each field at a magnification of 400×. The numbers of myelinated axons (b) and neural areas (c) from six or seven fields were summed. The total number of myelinated axons in each specimen was estimated as $b \times a/c$. Ultrathin sections of the same tissues stained with uranyl acetate (MERCK) and lead citrate (Nacalai Tesque) were examined via transmission electron microscopy (TEM) at a magnification

of 2,000×, using a model H-7000 microscope (Hitachi, Tokyo, Japan) equipped with an image acquisition system, to assess nerve fiber diameters (NFDs) and axon diameters (ADs). Photographs of 10 random fields from each ultrathin nerve section were analyzed using ImageJ[19–21]. Myelin thickness (MT) and g-ratio were calculated according to the formulas (NFD − AD)/2 and AD/NFD, respectively.

Evaluation of the Differentiation of the BM-MSCs Seeded in the Tube Containing Sural Vessels and a DANM (VBD Group)

Six rats from the VBD group were used in this experiment. Transplanted BM-MSCs were traced using a genetic labeling technique and a chemical marker. Three rats were seeded with BM-MSCs that were obtained from a Lewis-based green fluorescent protein (GFP) rat [LEW-Tg(CAG-EGFP)1Ys] strain[22] (provided by the National BioResource Project for the Rat in Japan). The remaining three rats were transplanted with BM-MSCs that had been labeled before transplantation with the chloromethylbenzamido dialkyl indocarbocyanine fluorescent dye (CM-DiI; Invitrogen, Carlsbad, CA, USA).

At 6 weeks, the midportions of the conduits were removed. Transverse frozen sections (thickness, 16 μm) were prepared as described above. Chicken monoclonal anti-GFP antibodies (1:200; Abcam, Cambridge, UK), rabbit polyclonal anti-glial fibrillary acidic protein (GFAP) antibodies (1:200; Merck Millipore, Darmstadt, Germany), and rabbit polyclonal anti-S-100 protein antibodies (1:500; Dako, Carpinteria, CA, USA) were used as primary antibodies. Donkey anti-chicken IgG (H+L) whole antibodies [1:200; CF^{TM}488 fluorescent reagents (for GFP); Biotium] and donkey anti-rabbit IgG (H+L) whole antibodies [1:200; CF^{TM}543 fluorescent reagents (for S-100 and GFAP); Biotium] were used as secondary antibodies in the sections from the rats that were seeded with BM-MSCs obtained from the GFP rat. Donkey anti-rabbit IgG (H+L) whole antibodies [1:200; CF^{TM}488 fluorescent reagents (for GFAP) and CF^{TM}350 fluorescent reagents (for S-100); Biotium] were used as secondary antibodies in the sections from the rats that were transplanted with CM-DiI-labeled BM-MSCs. The percentage of merged cells among the CM-DiI$^+$ cells was calculated using five random high-power fields per section.

Statistical Analyses

All data were expressed as the mean ± standard deviation (SD). The data from the CD8$^+$ cell counting experiment were analyzed using one-way analysis of variance (ANOVA) followed by a Tukey–Kramer test (JMP 8; SAS Institute, Cary, NC, USA). The data from electrophysiological, reinnervated muscle weight, and morphometric measurements were compared using an unpaired *t*-test. Values of $p<0.05$ were considered statistically significant.

RESULTS

Evaluation of the Revascularization of the DANM in the VCT (VD Group vs. D Group)

At 5 days, most of the RECA-1$^+$ cells were located around the vessels, and a few cells were observed only at the border and periphery of the DANM in the VD group; in contrast, almost no RECA-1$^+$ cells were found in the D group. In the VD group, RECA-1$^+$ cells were observed in the DANM around the inserted vessels at 1 week, and they had spread diffusely in the DANM at 4 weeks. In contrast, in the D group, only a few RECA-1$^+$ cells were observed exclusively in the peripheral region of the DANM at 4 weeks (Fig. 2).

Evaluation of the Immunogenicity of the DANM in the VCT (VD Group vs. Auto Group vs. Allo Group)

Immunohistochemistry revealed the presence of a much smaller number of CD8a$^+$ cells in the VD group compared with the allo group at each time point. The number of CD8a$^+$ cells in the VD, auto, and allo groups at a magnification of 200× was, respectively, 24±7, 45±13, and 151±45 per field at 2 weeks, and 21±6, 51±21, and 102±34 per field at 4 weeks. At both time points, there were significant differences between the VD and allo groups ($p<0.05$ at both time points), whereas no significant differences were detected between the VD and auto groups ($p=0.43$ at 2 weeks and $p=0.15$ at 4 weeks) (Fig. 3).

Evaluation of Nerve Regeneration Through the BM-MSC-Supplemented VCT With or Without DANM Implantation (VBD Group vs. VB Group)

Electrophysiological Evaluations. In the VBD group, CMAPs were detected in the pedal adductor muscles in all rats at 12 and 24 weeks. In contrast, in the VB group, CMAPs were not detected after stimulation at the S2 point (popliteal fossa) in four rats at 12 weeks and in three rats at 24 weeks. Because it was impossible to calculate the MNCV in seven rats, these animals were excluded from the evaluation of MNCV; thus, four rats at 12 weeks and five rats at 24 weeks were evaluated for MNCV in the VB group. The CMAP amplitudes in the VBD group were significantly higher than those observed in the VB group both at 12 weeks (10.1±6.4% vs. 3.6±2.5%, $p<0.05$) and at 24 weeks (69.3±16.6% vs. 10.6±9.0%, $p<0.05$). Although there were no significant differences between the VBD and VB groups at 12 or 24 weeks, there was a tendency for a faster MNCV in the VBD group versus the VB group at both time points (50.3±16.7% vs. 38.3±23.8%, $p=0.41$ at 12 weeks and 62.9±9.4% vs. 55.0±8.8%, $p=0.13$ at 24 weeks) (Fig. 4).

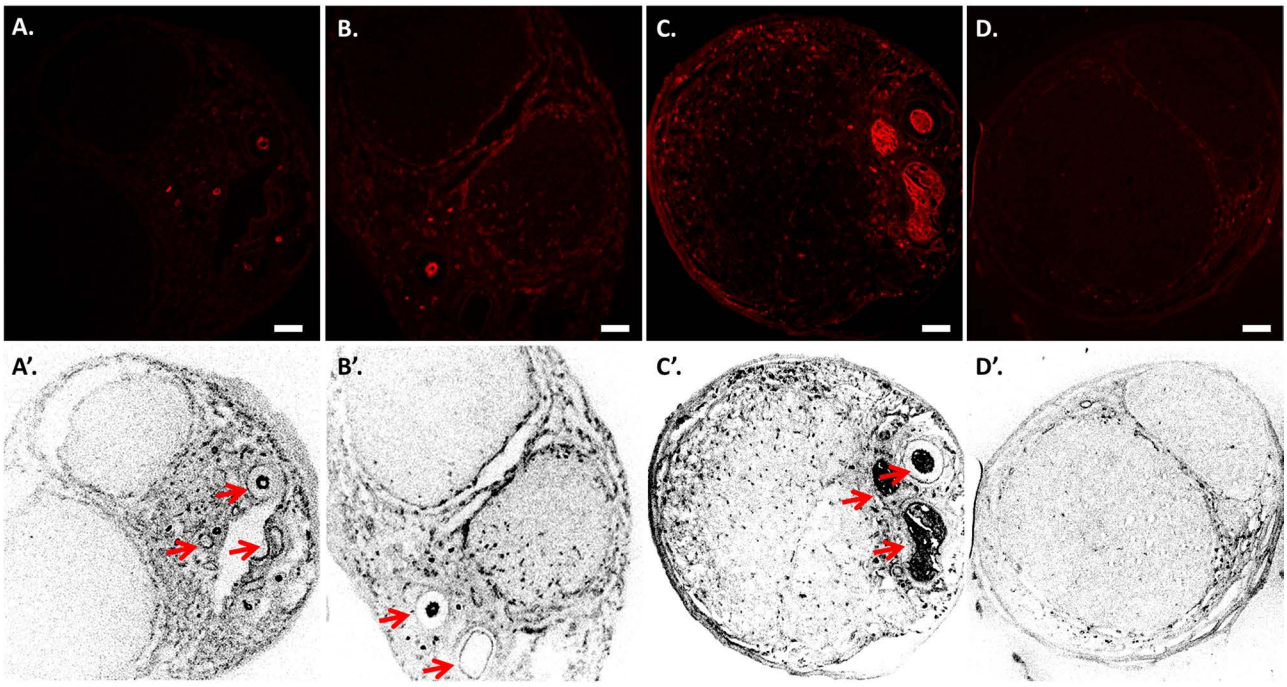

Figure 2. Revascularization of the decellularized allogenic nerve matrix (DANM). Immunohistochemistry for mouse monoclonal anti-rat endothelial cell cytoplasmic antigen (RECA-1) was performed on the transverse sections obtained from the midportion of the tube in the VD group at 5 days (A, A′), at 1 week (B, B′), and at 4 weeks (C, C′) and in the D group at 4 weeks (D, D′). (A, A′) A few RECA-1$^+$ cells were detected only at the periphery of the DANM, and no RECA-1$^+$ cells were observed inside the DANM at 5 days. (B, B′) RECA-1$^+$ cells were observed in the DANM at 1 week. The revascularized area was located mainly beside the inserted sural vessels. (C, C′, D, and D′) At 4 weeks, the RECA-1$^+$ cells had spread diffusely in the DANM in the VD group (C, C′), whereas RECA-1$^+$ cells were not found in the DANM in the D group (D, D′). The arrows indicate the inserted vascular bundle. Scale bars: 100 μm. VD group, the group with implantation of the sural vessels and a decellularized allogenic nerve matrix.

Reinnervated Muscle Weight. The wet muscle weight in the VBD group was significantly greater than that detected in the VB group at both time points (39.8±6.4% vs. 21.9±9.1%, $p<0.05$ at 12 weeks and 69.3±6.0% vs. 28.6±8.8%, $p<0.05$ at 24 weeks) (Fig. 4).

Histological and Morphometric Evaluations. In both groups, the arteriovenous bundle that had been inserted into the tube, as well as neural tissues with many well-myelinated axons, was observed in semithin transverse sections. The red blood cells found inside the lumen of the vessels indicated the patency of the vascular vessels. Many remyelinated axons were observed in the VBD group, whereas neural tissues were mainly formed around the inserted vascular pedicle in the VB group (Fig. 5A–H). TEM revealed the presence of remyelinated axons with proper myelin sheaths in both groups (Fig. 5I–L). The morphometric analysis showed that the VBD group had a significantly larger number of myelinated axons (3,370±1,253 vs. 852±435, $p<0.05$ at 12 weeks and 4,650±722 vs. 2,324±1,035, $p<0.05$ at 24 weeks), significantly larger neural areas (0.41±0.09 mm^2 vs. 0.20±0.14 mm^2, $p<0.05$ at 12 weeks and 0.60±0.11 mm^2 vs. 0.26±0.11 mm^2, $p<0.05$ at 24 weeks), a significantly greater MT (0.58±0.04 μm vs. 0.45±0.09 μm, $p<0.05$ at 12 weeks and 0.63±0.08 μm vs. 0.49±0.04 μm, $p<0.05$ at 24 weeks), and significantly larger NFDs (3.47±0.37 μm vs. 2.89±0.36 μm, $p<0.05$ at 12 weeks and 3.88±0.53 μm vs. 3.09±0.27 μm, $p<0.05$ at 24 weeks) than did the VB group at both time points (Fig. 5M–P). The g-ratios in the VBD and VB groups were, respectively, 0.63±0.03 and 0.66±0.02 at 12 weeks, and 0.63±0.03 and 0.66±0.03 at 24 weeks. These g-ratio values were all within the optimal range[23].

Differentiation of the Implanted Cells in the VBD Group

GFP$^+$ cells and CM-DiI-labeled cells were observed in DANMs, indicating that the BM-MSCs that were transplanted around the DANMs migrated into DANMs and survived for 6 weeks. Some of the GFP$^+$ cells and the CM-DiI$^+$ cells were also immunopositive for S-100 and GFAP (Figs. 6 and 7), indicating that the BM-MSCs were induced to differentiate into SC-like cells in the DANMs in VCTs. The percentage of cells in which CM-DiI was colocalized with S-100 and GFAP among the CM-DiI$^+$ cells was 31.8% and 28.8%, respectively.

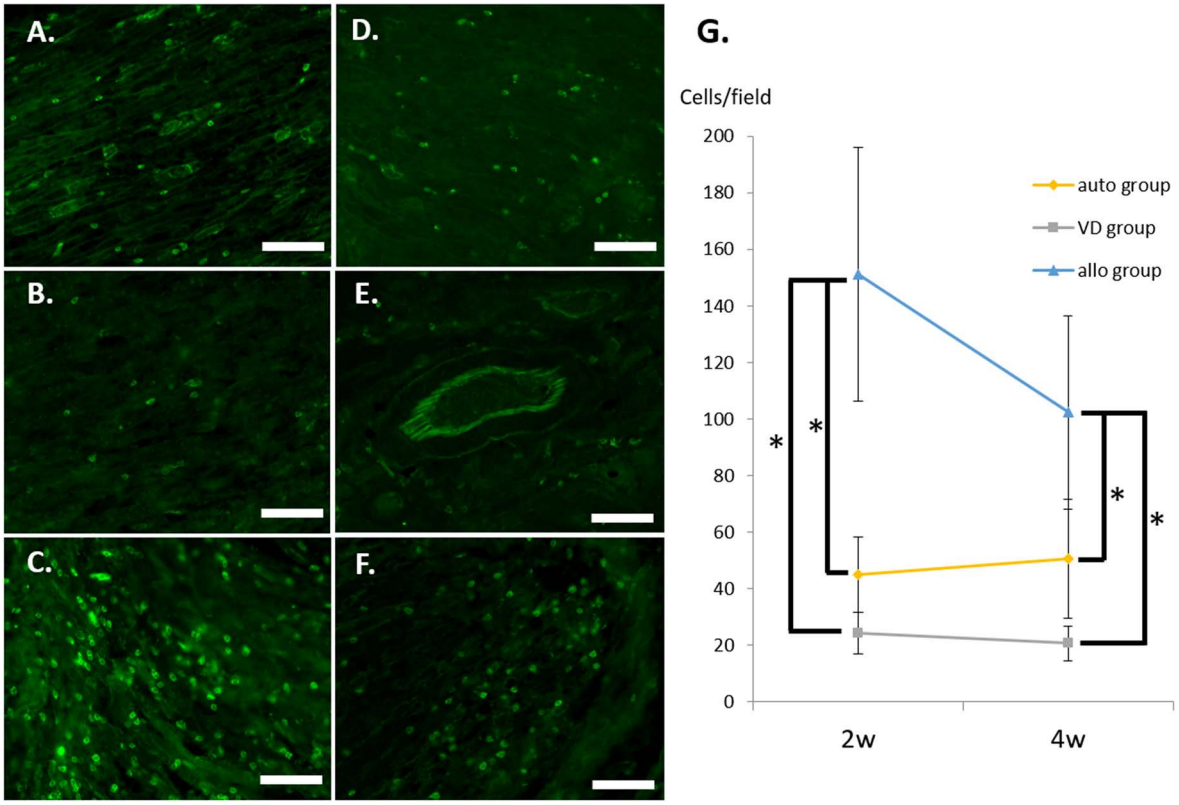

Figure 3. Immunogenicity of the grafts. Longitudinal sections of the distal part of the bridging materials were investigated in the auto group (A, D), the VD group (B, E), and the allo group (C, F) at 2 (A–C) and 4 (D–F) weeks using immunohistochemistry for CD8. The number of $CD8^+$ cells was determined per field, and quantification is shown (G). Scale bars: 100 μm. *$p<0.01$. VD group, the group with implantation of the sural vessels and a decellularized allogenic nerve matrix.

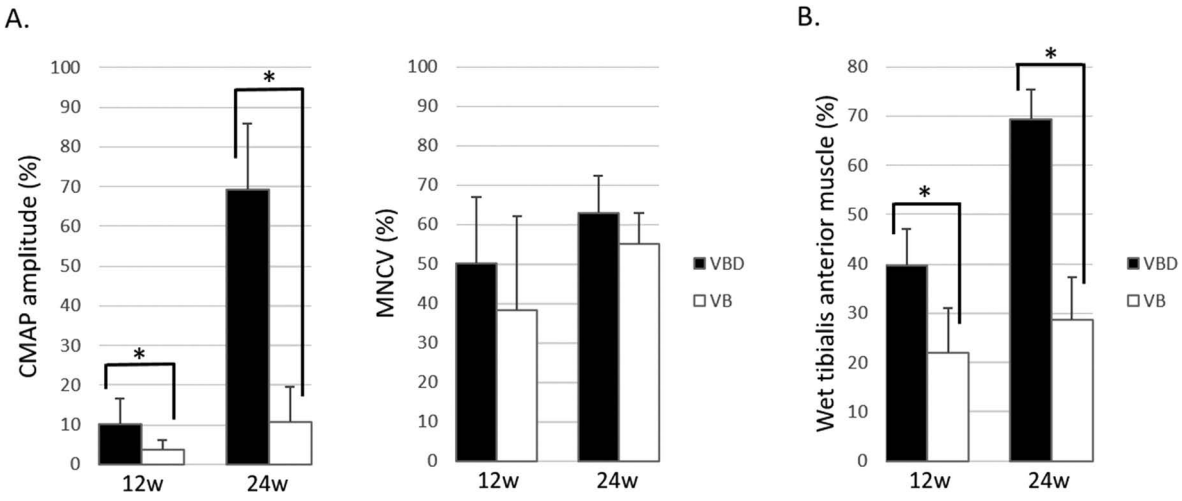

Figure 4. Electrophysiological studies and reinnervated muscle weight measurements (VBD group vs. VB group). The VBD group was significantly superior to the VB group regarding compound muscle action potential (CMAP) amplitude (A) and wet tibialis anterior muscle weight (B) at both 12 and 24 weeks. The data are presented as a percentage of the value recorded on the contralateral side. *$p<0.05$. MNCV, motor nerve conduction velocity; VBD group, the group with implantation of the sural vessels, bone marrow-derived mesenchymal stem cells (BM-MSCs), and a decellularized allogenic nerve matrix (DANM); VB group, the group with the sural vessels and the BM-MSCs.

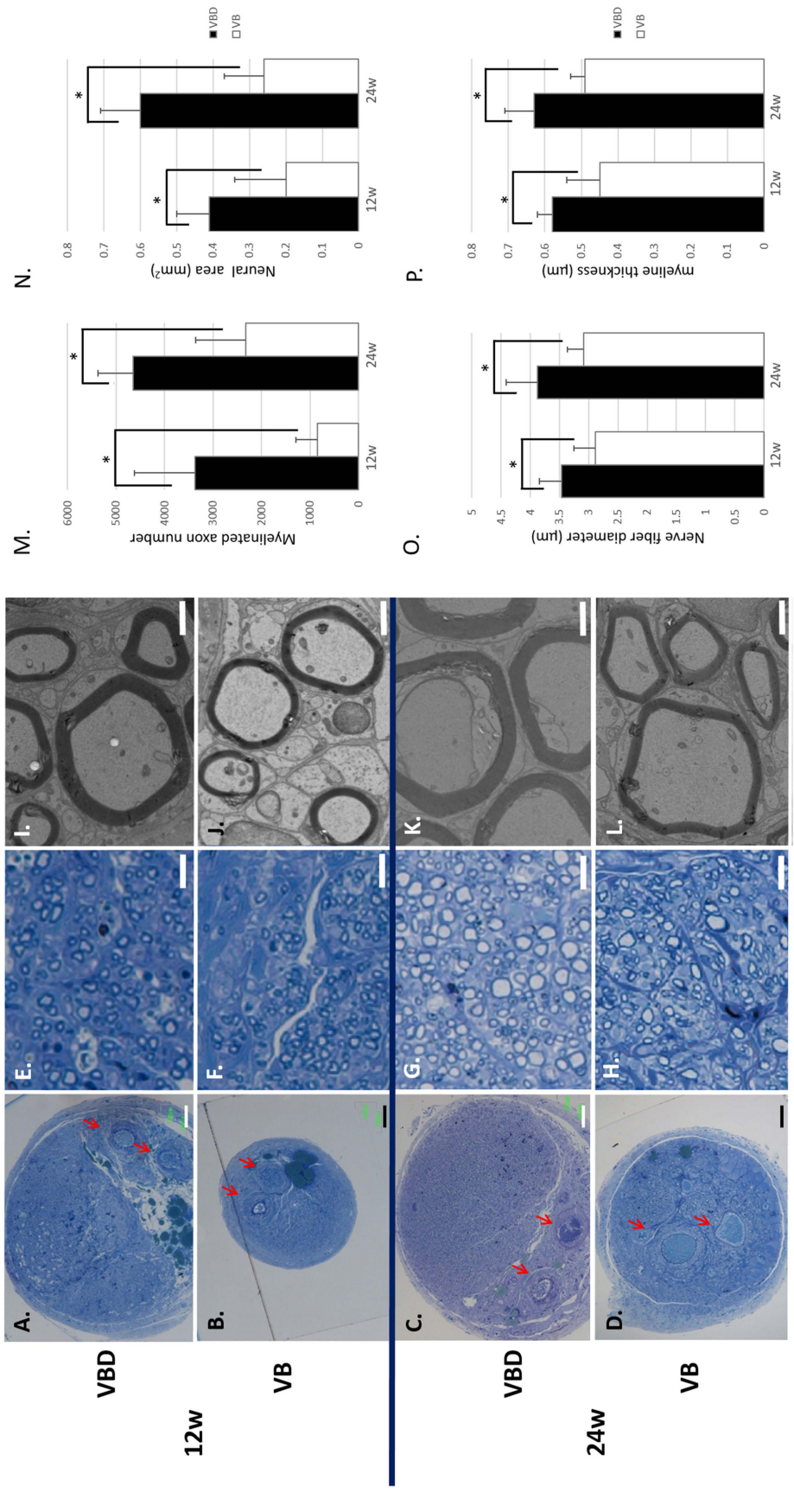

Figure 5. Histological and morphometric evaluations (VBD group vs. VB group). Transverse sections of the regenerated nerve 5 mm distal to the distal suture were observed under light microscopy (A–H) and transmission electron microscopy (TEM; I–L) at 12 (A, B, E, F, I, and J) and 24 (C, D, G, H, K, and L) weeks. Red blood cells filled the lumen of the inserted vessels (arrow). The number of myelinated axons (M) and the neural area (N) were larger in the VBD group compared with the VB group. Regenerated axons with a larger diameter (O) and thicker myelin sheaths (P) were observed in the VBD group compared with the VB group. Scale bars: 100 μm (A–D), 10 μm (E–H), and 2 μm (I–L). *$p<0.05$. VBD group, the group with implantation of the sural vessels, bone marrow-derived mesenchymal stem cells (BM-MSCs), and a decellularized allogenic nerve matrix (DANM); VB group, the group with the sural vessels and the BM-MSCs.

DISCUSSION

The current study showed that the addition of a thermal DANM as a scaffold for nerve regeneration to vessel-containing nerve tubes supplemented with BM-MSCs yielded optimized axonal regeneration, according to electrophysiological and morphometric parameters and wet tibialis anterior muscle weight measurements, when bridging a critical long nerve gap in rats. The DANM in the tube was revascularized by newly formed blood vessels that originated from the inserted vascular bundle and showed no harmful immunogenicity when transplanted alongside the arteriovenous bundle. The BM-MSCs that were transplanted around the DANM inside the lumen of the tube migrated into the DANM and survived for at least 6 weeks after transplantation. Moreover, some of the BM-MSCs that migrated into the DANM differentiated into Schwann cell-like cells.

An allogenic nerve matrix is a promising 3D scaffold because of its endoneurial microstructures with ECM and its availability without sacrificing healthy nerves. However, because of its cellular components, including Schwann cells, it produces severe immune reactions that hamper axonal regeneration. Using thermal decellularization, cells with problematic immunogenicity were removed from the allogenic nerve segment, while its ECM was preserved. Ide and colleagues reported serial studies that used higher mammalian models to show the usefulness of decellularized allogenic nerve segments as scaffolds in nerve regeneration[10,11]. However, the efficacy of the implantation of a DANM in VCTs is not well known; the mechanism underlying the formation of a neovascular network in the DANM in VCTs remains unknown, as does the level of immunogenicity of the DANM that is implanted alongside the vascular bundle.

Our immunohistochemical study of RECA-1, which is found in vascular endothelial cells, revealed that the DANM in the VCT was vascularized in the early posttransplantation period (5–7 days after surgery). Conversely, RECA-1$^+$ cells were hardly found in the midportion of the DANM in a simple silicone tube without a vascular bundle in the lumen, even at 4 weeks after surgery. These results indicate that the vascular vessels inserted into the tube played a key role in the extension of capillaries into the DANM in the VCT. Kakinoki et al. performed angiography on the VCT and demonstrated the formation of an intratubular capillary network around the inserted vessels[3]. The DANM in the VCT was considered to be revascularized by the inserted vascular bundle via the same mechanism. Several experimental and clinical findings reported recently indicate that new capillary formation is closely related to axonal elongation and regeneration[24–28]. The formation of a capillary network is

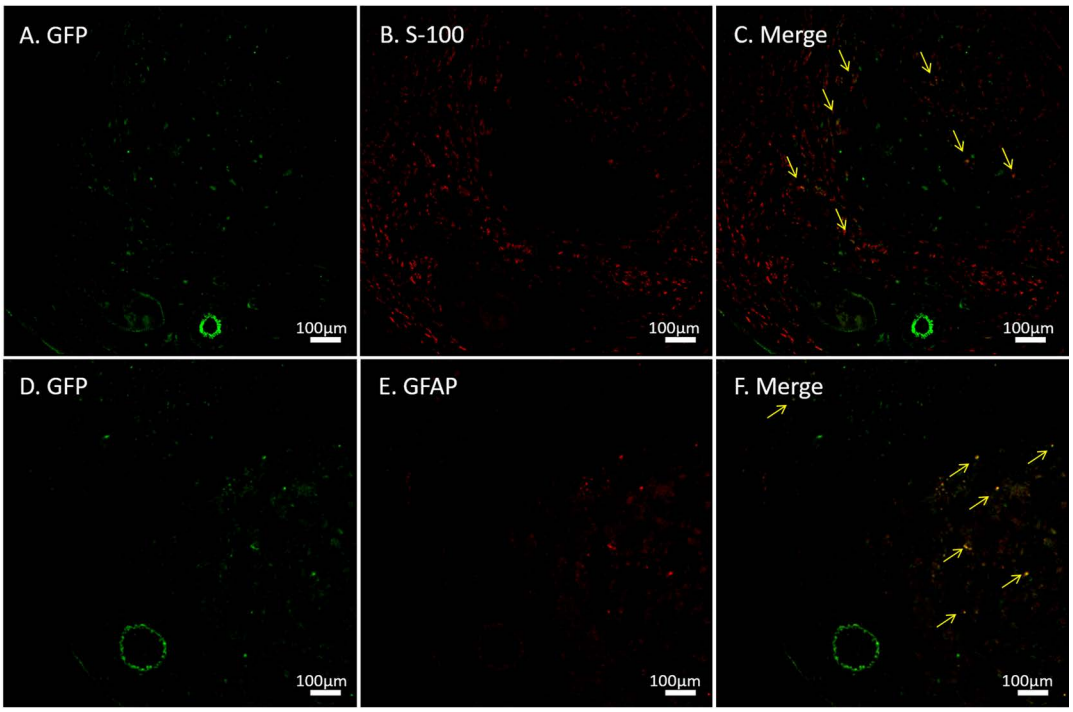

Figure 6. Immunohistochemistry for green fluorescent protein (GFP), S-100, and glial fibrillary acidic protein (GFAP). GFP$^+$ cells were observed at 6 weeks after transplantation into conduits containing a vascular bundle and a decellularized allogenic nerve matrix (DANM). Some of the implanted cells were immunopositive for S-100 (A–C) and GFAP (D–F). The arrows indicate the merged cells.

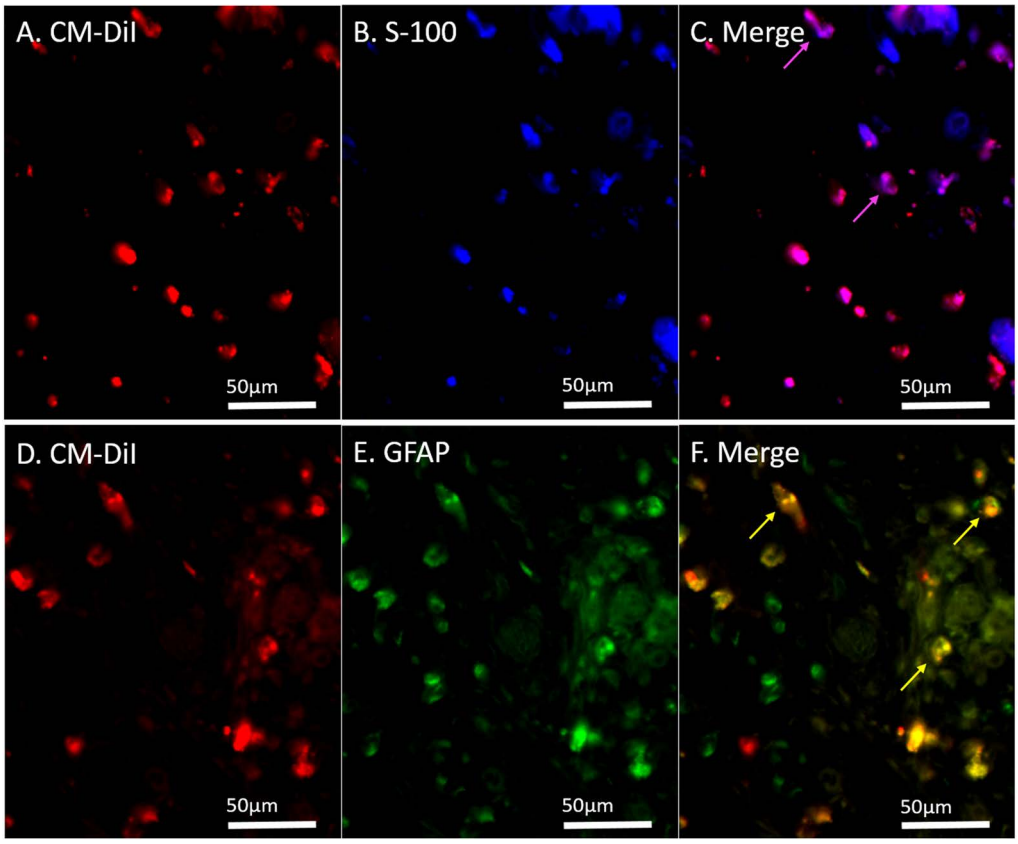

Figure 7. Immunohistochemistry for S-100 and glial fibrillary acidic protein (GFAP) after transplantation of the chloromethylbenzamido dialkyl indocarbocyanine fluorescent dye (CM-DiI)-labeled bone marrow-derived mesenchymal stem cells (BM-MSCs). CM-DiI$^+$ cells were detected in the decellularized allogenic nerve matrix (DANM) in the BM-MSC-seeded vessel-containing tube at 6 weeks after transplantation, and 31.8% and 28.8% of the CM-DiI$^+$ cells were immunopositive for S-100 (A–C) and GFAP (D–F), respectively. The arrows indicate the merged cells.

reportedly essential for subsequent Schwann cell-mediated axonal regeneration[29]. The early revascularization of the DANM in a VCT is of great advantage for peripheral nerve regeneration.

CD8$^+$ lymphocytes are mainly employed around the graft tissue in the acute phase of allogenic graft rejection[30]. Our immunohistochemistry results revealed that the number of CD8$^+$ cells observed in the DANM in the VCTs (VD group) was significantly smaller than that detected in the allogenic nerve segments (allo group) and was comparable to that observed in the autologous nerve segments (auto group) at 2 and 4 weeks after surgery. Moreover, the number of CD8$^+$ cells in the VD group tended to decrease between 2 and 4 weeks after transplantation. These findings indicate that the DANM in VCTs was immunologically tolerant in the acute phase.

In the current study, we only compared the VBD with the VB groups regarding axonal regeneration because our main purpose was to investigate whether the addition of DANM implantation to the BM-MSC-supplemented VCT (the VB group) would optimize peripheral nerve regeneration. To identify the mechanism underlying the optimization of the peripheral nerve regeneration in the conduit in the VBD group, the effect of BM-MSC implantation should be investigated. Thus, we added an additional eight rats to the VD group for the evaluation of the regenerated nerve and compared the VBD group with the VD group at 24 weeks (unpublished data). The electrophysiological examinations revealed the superiority of the VBD group versus the VD group, as the former exhibited a significantly higher CMAP amplitude (69.3±16.6% vs. 40.6±27.4%, $p=0.02$) and a significantly faster MNCV (62.9±9.4% vs. 41.9±11.6%, $p<0.01$). The number of myelinated axons in the VBD group was significantly larger than that detected in the VD group (4,650±722 vs. 3,030±900, $p<0.01$). The tibialis anterior muscle weight in the VBD group was also higher than that observed in the VD group, although not significantly (69.3±6.0% vs. 58.9±10.8%, $p=0.06$) (Fig. 8). These results indicate a positive effect of

BM-MSC implantation regarding nerve regeneration in the VBD group.

Mesenchymal stem cells are reportedly able to enhance neovascularization by producing angiopoietin-1 (Ang-1) and Ang-2, as well as Ang-like-1, -2, -3, and -4, vascular endothelial growth factor, and FGF-2[31–34], and to suppress an ongoing immune response by inhibiting T-cell proliferation[35–37]. Thus, it seems reasonable to assume that with the aid of BM-MSC implantation, the DANM in the BM-MSC-supplemented VCT is more quickly revascularized and exhibits less immunogenicity, resulting in the optimization of the regenerated nerve. Several other merits of the implantation of BM-MSCs into nerve conduits have been reported, including an autocrine ability (production and secretion of neurotrophic and neurotropic factors)[38–41] and the differentiation of the BM-MSCs themselves into Schwann cell-like cells in the nerve conduit[4,5,14,42,43]. Although the results of our immunohistochemistry experiment also support this ability of BM-MSCs to differentiate into Schwann cell-like cells, some researchers have claimed that cellular fusion between implanted cells and resident cells occurs rather than real transdifferentiation[44,45]. Whether BM-MSCs differentiate into Schwann cell-like cells without fusion remains to be addressed.

Cells, scaffolds, and growth factors are essential for tissue regeneration. From this perspective, the current nerve conduit was ideal: it contained BM-MSCs as a cellular component; a DANM as a scaffold; and several neurotrophic and neurotropic factors that were released from the nerve stumps, the implanted BM-MSCs, and the cells that moved from the nerve stumps, including Schwann cells, macrophages, and fibroblasts, as growth factors. The appropriate administration of additional growth factors into nerve conduits would allow even greater nerve regeneration. However, many problems remain to be solved before undertaking the additional application of growth factors to nerve conduits, including the determination of the ideal dose, timing, and method of delivery of these factors.

A modification of the cell delivery method should be performed to maximize the favorable effects of BM-MSC implantation. We injected cells in medium into the lumen of the tube, rather than into the DANM directly, for the following reasons. First, the DANM exhibited swelling after the injection of the cells in medium into the DANM directly. A swollen DANM would increase the risk of occlusion of the sural vessels that were introduced into the silicone tube as a source of vascularity. Second, the direct injection technique may damage the ECM structure of the DANM. Third, our fluoroscopy experiment demonstrated that prelabeled implanted cells were detected inside the DANM at 6 weeks after implantation, which suggests that the cells that had been seeded around the DANM migrated into the DANM probably through the degenerated epineurium and both suture sites. Finally, injection into the lumen of the tube is easier to perform compared with direct injection into the DANM. However, our method of implantation of the cells was also associated with several drawbacks, including leakage of the implanted cells and the necessity of cell migration into the DANM. A more efficient method of transplantation of cells into the regenerating nerve needs to be developed in the future.

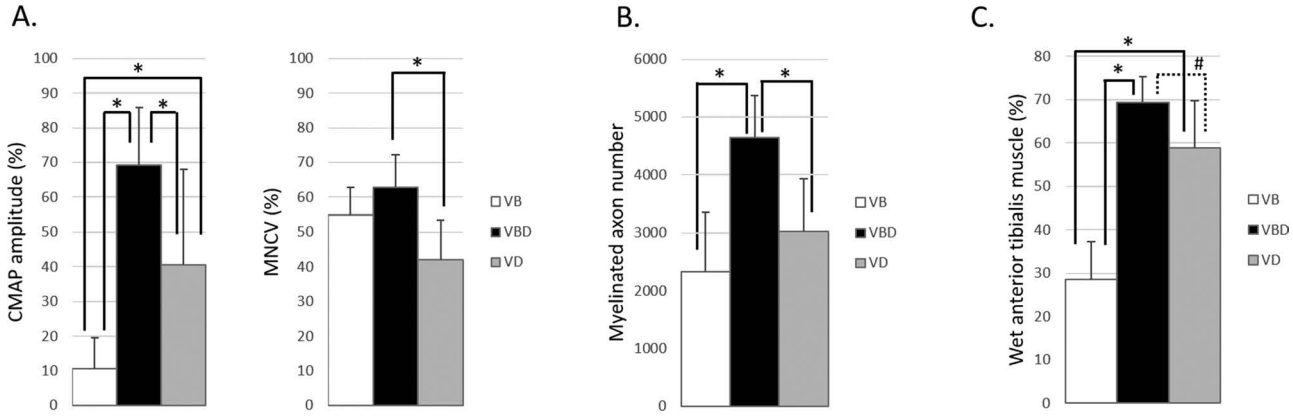

Figure 8. Comparison of the regenerated nerve at 24 weeks (including the VD group, $n=8$ in each group). The comparison among the VB, VBD, and VD groups at 24 weeks revealed that the VBD group was significantly superior not only to the VB group but also to the VD group regarding electrophysiological and morphometric measurements. The data obtained from electrophysiological studies (A) and reinnervated muscle weight measurements (C) are presented as a percentage of the value recorded on the contralateral side. The data were analyzed by one-way analysis of variance (ANOVA) followed by a Tukey–Kramer test. $*p<0.05$ and $\#p=0.06$. CMAP, compound muscle action potential, MNCV, motor nerve conduction velocity; VB group, the group with the sural vessels and the bone marrow-derived mesenchymal stem cells (BM-MSCs); VBD group, the group with implantation of the sural vessels, the BM-MSCs, and a decellularized allogenic nerve matrix (DANM); VD group, the group with implantation of the sural vessels and a DANM.

In this study, we used a rodent sciatic nerve model that is generally approved and conventionally used in basic research on peripheral nerve regeneration. However, rodents demonstrate superior neuroregenerative capacity compared with humans and higher mammals. Therefore, the present results may not be applicable in clinical settings. The current study lacked a comparison with autografts regarding the assessment of the regenerated nerve, which was also a limitation of this study.

In conclusion, our novel nerve conduit, a BM-MSC-supplemented VCT with transplantation of a DANM, created a chamber with an optimal environment for peripheral nerve regeneration. The DANM in the VCT provided an immunologically tolerated 3D scaffold that was vascularized in the early posttransplantation phase by the rapid formation of a capillary network from the inserted vascular bundle. Scaffolds with vascularity can promote the survival rate of implanted BM-MSCs, which exhibit various abilities to improve the efficacy of cell therapy, namely, trophic effects, angiogenesis, and immune modulation. A VCT with implantation of BM-MSCs and of a DANM is expected to be a promising option for peripheral nerve repair without the use of immunosuppressant drugs.

ACKNOWLEDGMENTS: This work was supported by a Grant-in-Aid for Scientific Research (26462240) from the Japan Society for the Promotion of Science. The authors would like to express their great appreciation to Ms. Keiko Furuta (Division of Electron Microscopic Study, Center for Anatomical Studies, Graduate School of Medicine, Kyoto University) for her help in histological studies. The authors declare no conflicts of interest.

REFERENCES

1. Meek MF, Coert JH. US Food and Drug Administration/Conformit Europe-approved absorbable nerve conduits for clinical repair of peripheral and cranial nerves. Ann Plast Surg. 2008;60:110–6.
2. Ray WZ, Mackinnon SE. Management of nerve gaps: Autografts, allografts, nerve transfers, and end-to-side neurorrhaphy. Exp Neurol. 2010;223:77–85.
3. Kakinoki R, Nishijima N, Ueba Y, Oka M, Yamamuro T. Relationship between axonal regeneration and vascularity in tubulation—An experimental study in rats. Neurosci Res. 1995;23:35–45.
4. Yamakawa T, Kakinoki R, Ikeguchi R, Nakayama K, Morimoto Y, Nakamura T. Nerve regeneration promoted in a tube with vascularity containing bone marrow-derived cells. Cell Transplant. 2007;16:811–22.
5. Kaizawa Y, Kakinoki R, Ikeguchi R, Ohta S, Noguchi T, Oda H, Matsuda S. Bridging a 30 mm defect in the canine ulnar nerve using vessel-containing conduits with implantation of bone marrow stromal cells. Microsurgery 2016;36:316–24.
6. Fansa H, Keilhoff G, Plogmeier K, Frerichs O, Wolf G, Schneider W. Successful implantation of Schwann cells in acellular muscles. J Reconstr Microsurg. 1999;15:61–65.
7. Gulati AK, Cole GP. Nerve graft immunogenicity as a factor determining axonal regeneration in the rat. J Neurosurg. 1990;72:114–22.
8. Hall SM. Regeneration in cellular and acellular autografts in the peripheral nervous system. Neuropathol Appl Neurobiol. 1986;12:27–46.
9. Ide C, Tohkyama K, Yokota R, Nitatori T, Onodera S. Schwann cell basal lamina and nerve regeneration. Brain Res. 1983;288:61–75.
10. Ide C, Tohyama K, Tajima K, Endoh K, Sano K, Tamura M, Mizoguchi A, Kitada M, Morihara T, Shirasu M. Long acellular nerve transplants for allogeneic grafting and the effects of basic fibroblast growth factor on the growth of regenerating axons in dogs: A preliminary report. Exp Neurol. 1998;154:99–112.
11. Tajima K, Tohyama K, Ide C, Abe M. Regeneration through nerve allografts in the cynomolgus monkey (Macaca fascicularis). J Bone Joint Surg Am. 1991;73:172–85.
12. Lassner F, Schaller E, Steinhoff G, Wonigeit K, Walter GF, Berger A. Cellular mechanisms of rejection and regeneration in peripheral nerve allografts. Transplantation 1989;48:386–92.
13. Tohill M, Mantovani C, Wiberg M, Terenghi G. Rat bone marrow mesenchymal stem cells express glial markers and stimulate nerve regeneration. Neurosci Lett. 2004;362:200–3.
14. Nijhuis TH, Brzezicki G, Klimczak A, Siemionow M. Isogenic venous graft supported with bone marrow stromal cells as a natural conduit for bridging a 20 mm nerve gap. Microsurgery 2010;30:639–45.
15. Siemionow M, Duggan W, Brzezicki G, Klimczak A, Grykien C, Gatherwright J, Nair D. Peripheral nerve defect repair with epineural tubes supported with bone marrow stromal cells: A preliminary report. Ann Plast Surg. 2011;67:73–84.
16. Jesuraj NJ, Santosa KB, Newton P, Liu Z, Hunter DA, Mackinonn SE, Sakiyama-Elbert SE, Johnson PJ. A systematic evaluation of Schwann cell injection into acellular cold-preserved nerve grafts. J Neurosci Methods 2011;197:209–15.
17. Ikeguchi R, Kakinoki R, Matsumoto T, Hyon SH, Nakamura T. Peripheral nerve allografts stored in green tea polyphenol solution. Transplantation 2005;79:688–95.
18. Matsumoto T, Kakinoki R, Ikeguchi R, Hyon SH, Nakamura T. Optimal conditions for peripheral nerve storage in green tea polyphenol: An experimental study in animals. J Neurosci Methods 2005;145:255–66.
19. Gu Y, Zhu J, Xue C, Li Z, Ding F, Yang Y, Gu X. Chitosan/silk fibroin-based, Schwann cell-derived extracellular matrix-modified scaffolds for bridging rat sciatic nerve gaps. Biomaterials 2014;35:2253–63.
20. Wang Y, Zhao Z, Ren Z, Zhao B, Zhang L, Chen J, Xu W, Lu S, Zhao Q, Peng J. Recellularized nerve allografts with differentiated mesenchymal stem cells promote peripheral nerve regeneration. Neurosci Lett. 2012;514:96–101.
21. Yang XN, Jin YQ, Bi H, Wei W, Cheng J, Liu ZY, Shen Z, Qi ZL, Cao Y. Peripheral nerve repair with epimysium conduit. Biomaterials 2013;34:5606–16.
22. Inoue H, Ohsawa I, Murakami T, Kimura A, Hakamata Y, Sato Y, Kaneko T, Takahashi M, Okada T, Ozawa K, Francis J, Kobayashi E. Development of new inbred transgenic strains of rats with LacZ or GFP. Biochem Biophys Res Commun. 2005;329:288–95.
23. Chomiak T, Hu B. What is the optimal value of the g-ratio for myelinated fibers in the rat CNS? A theoretical approach. PLos One 2009;4:e7754.
24. Hobson MI, Green CJ, Terenghi G. VEGF enhances intraneural angiogenesis and improves nerve regeneration after axotomy. J Anat. 2000;197:591–605.

25. Ozcan G, Shenaq S, Mirabi B, Spira M. Nerve regeneration in a bony bed: Vascularized versus nonvascularized nerve grafts. Plast Reconstr Surg. 1993;91:1322–31.
26. Podhajsky RJ, Myers RR. The vascular response to nerve crush: Relationship to Wallerian degeneration and regeneration. Brain Res. 1993;623:117–23.
27. Weerasuriya A. Patterns of change in endoneurial capillary permeability and vascular space during nerve regeneration. Brain Res. 1990;510:135–9.
28. Zhu Y, Liu S, Zhou S, Yu Z, Tian Z, Zhang C, Yang W. Vascularized versus nonvascularized facial nerve grafts using a new rabbit model. Plast Reconstr Surg. 2015;135: 331e–9e.
29. Cattin AL, Burden JJ, Van Emmenis L, Mackenzie FE, Hoving JJ, Garcia Calavia N, Guo Y, McLaughlin M, Rosenberg LH, Quereda V, Jamecna D, Napoli I, Parrinello S, Enver T, Ruhrberg C, Lloyd AC. Macrophage-induced blood vessels guide Schwann cell-mediated regeneration of peripheral nerves. Cell 2015;162:1127–39.
30. Sayegh MH, Turka LA. The role of T-cell costimulatory activation pathways in transplant rejection. N Engl J Med. 1998;338:1813–21.
31. Phinney DG. Biochemical heterogeneity of mesenchymal stem cell populations: Clues to their therapeutic efficacy. Cell Cycle 2007;6:2884–9.
32. Hsiao ST, Asgari A, Lokmic Z, Sinclair R, Dusting GJ, Lim SY, Dilley RJ. Comparative analysis of paracrine factor expression in human adult mesenchymal stem cells derived from bone marrow, adipose, and dermal tissue. Stem Cells Dev. 2012;21:2189–203.
33. Kira T, Omokawa S, Akahane M, Shimizu T, Nakano Y, Onishi T, Kido A, Inagaki Y, Tanaka Y. Effectiveness of bone marrow stromal cell sheets in maintaining random-pattern skin flaps in an experimental animal model. Plast Reconstr Surg. 2015;136:624e–32e.
34. Yang Z, Cai X, Xu A, Xu F, Liang Q. Bone marrow stromal cell transplantation through tail vein injection promotes angiogenesis and vascular endothelial growth factor expression in cerebral infarct area in rats. Cytotherapy 2015;17:1200–12.
35. Aggarwal S, Pittenger MF. Human mesenchymal stem cells modulate allogeneic immune cell responses. Blood 2005;105:1815–22.
36. Bartholomew A, Sturgeon C, Siatskas M, Ferrer K, McIntosh K, Patil S, Hardy W, Devine S, Ucker D, Deans R, Moseley A, Hoffman R. Mesenchymal stem cells suppress lymphocyte proliferation in vitro and prolong skin graft survival in vivo. Exp Hematol. 2002;30:42–8.
37. Di Nicola M, Carlo-Stella C, Magni M, Milanesi M, Longoni PD, Matteucci P, Grisanti S, Gianni AM. Human bone marrow stromal cells suppress T-lymphocyte proliferation induced by cellular or nonspecific mitogenic stimuli. Blood 2002;99:3838–43.
38. Chen CJ, Ou YC, Liao SL, Chen WY, Chen SY, Wu CW, Wang CC, Wang WY, Huang YS, Hsu SH. Transplantation of bone marrow stromal cells for peripheral nerve repair. Exp Neurol. 2007;204:443–53.
39. Crigler L, Robey RC, Gaupp D, Phinney DG, Asawachaicharn A. Human mesenchymal stem cell subpopulations express a variety of neuro-regulatory molecules and promote neuronal cell survival and neuritogenesis. Exp Neurol. 2006;198:54–64.
40. Wang J, Ding F, Gu Y, Liu J, Gu X. Bone marrow mesenchymal stem cells promote cell proliferation and neurotrophic function of Schwann cells in vitro and in vivo. Brain Res. 2009;1262:7–15.
41. Zhao Z, Wang Y, Peng J, Ren Z, Zhang L, Guo Q, Xu W, Lu S. Improvement in nerve regeneration through a decellularized nerve graft by supplementation with bone marrow stromal cells in fibrin. Cell Transplant. 2014;23: 97–110.
42. Jia H, Wang Y, Tong XJ, Liu GB, Li Q, Zhang LX, Sun XH. Sciatic nerve repair by acellular nerve xenografts implanted with BMSCs in rats xenograft combined with BMSCs. Synapse 2012;66:256–69.
43. Cuevas P, Carceller F, Dujovny M, Garcia-Gómez I, Cuevas B, González-Corrochano R, Diaz-González D, Reimers, D. Peripheral nerve regeneration by bone marrow stromal cells. Neurol Res. 2002;24:634–8.
44. Weimann, JM, Charlton, CA, Brazelton, TR, Hackman, RC, Blau HM. Contribution of transplanted bone marrow cells to Purkinje neurons in human adult brains. Proc Natl Acad Sci USA 2003;100:2088–93.
45. Spees JL, Olson SD, Ylostalo J, Lynch PJ, Smith J, Perry A, Peister A, Wang MY, Prockop DJ. Differentiation, cell fusion, and nuclear fusion during ex vivo repair of epithelium by human adult stem cells from bone marrow stroma. PNAS 2003;100:2397–402.